Model of the electronic-vibrational kinetics of O_2 and O_3 photolysis in the Earth's middle atmosphere: analysis of sensitivity

V.A. Kuleshova and V.A. Yankovsky

V.A. Fok Research & Development Institute of Physics,
St. Petersburg State University, Petrodvorets

Received October 3, 2006

The sensitivity of the model of electronic-vibrational kinetics of O_2 and O_3 photolysis [V.A. Yankovsky and R.O. Manuilova, Atmos. Oceanic Opt. **16**, No. 7, 536–540 (2003)] to variations of basic components of mesosphere and lower thermosphere and to reaction rate constants has been studied both in the direct problem of calculation of vertical concentration profiles of $O_2(b^1\Sigma_g^+, v = 0–2)$ and $O_2(a^1\Delta_g, v = 0–5)$ and in the inverse problem of vertical O_3 profile retrieval from the intensities of emissions of Atm (0–0) (762 nm) and IR Atm (0–0) (1.27 μm) O_2 bands. The interrelation is shown between the error of calculations of vertical concentration profiles of $O_2(b^1\Sigma_g^+, v = 0–2)$ and $O_2(a^1\Delta_g, v = 0–5)$, recovered vertical O_3 profile, and other output model parameters with the factors of model sensitivity to input parameters and their fractional errors. Groups of key atmospheric parameters and aeronomic reactions for each task have been specified. Significant dependence of vertical O_3 profile retrieval from the Atm (0–0) O_2 emission intensity on CO_2 concentration profile at altitudes from 65 to 90 km has been established.

Introduction

The up-to-date YM-2003 photochemical model of ozone and molecular oxygen dissociation was published in 2003. This work continues a series of works,[1–3] studying properties of the new model which, as against previous ones,[4,5] takes into account the formation of electronic-vibrationally excited oxygen molecules both at O_2 and O_3 photodissociation and in processes of energy exchange between photolytes. The schematic of processes in the YM-2003 models are shown in Fig. 1.

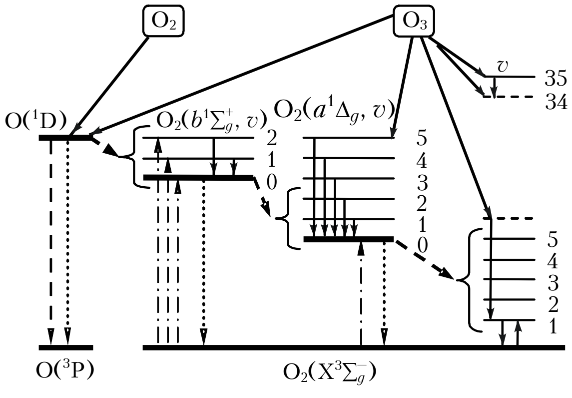

Fig. 1. Schematic of formation of daytime emissions of $O_2(a^1\Delta_g, v \geq 0)$ and $O_2(b^1\Sigma_g^+, v \geq 0)$ in the middle atmosphere in the YM-2003 model: photolytic populating (thick solid lines); collisional quenching (thick dashed lines); EE exchange processes (thin solid lines); resonance photoexcitation (dash-dotted lines); radiative quenching (dotted lines).

This model first takes into account the resonance absorption of solar radiation in 688 and 629 nm bands by oxygen molecules, resulting in populating of electronic-vibrational excited states of the $O_2(b^1\Sigma_g^+, v = 1, 2)$ molecule, respectively, and formation of electronic-vibrational exited $O_2(a^1\Delta_g, v = 0–5)$ molecules at ozone photolysis in the Hartley band. Since the model takes into account more than 100 different aeronomic reactions (photolytic and resonance populating, radiative quenching, and collisional energy transfer between the oxygen molecule levels), then the question arises of sensitivity of the model to variations of kinetic parameters, i.e., atmospheric component concentrations, gas temperature, chemical reaction rate constants, known with different degrees of uncertainty.

Sensitivities of previous models of O_2 and O_3 photodissociation were analyzed in Refs. 4–7, but these studies were incomplete.

The sensitivity of one of the first ozone dissociation model to solar flux variations at different Sun zenith angles was analyzed under twilight conditions in Ref. 4. The sensitivity of the model to variations of reaction rate constants was not analyzed, a number of processes important for atmospheric photochemistry was not either considered [molecular oxygen photodissociation in the Schumann–Runge continuum and Lyman-α band, resulting in excitement of $O(^1D)$ atoms, which is a key point for altitudes higher than 80 km; atomic-oxygen quenching of the second singlet level of the $O_2(b^1\Sigma_g^+, v = 0)$ by the atomic oxygen].

As compared to the above model, the O_2 and O_3 photodissociation model for daylight conditions[5] was supplemented with molecular oxygen photolysis processes; this allowed a relative increase of ozone concentration in Earth's mesosphere and lower thermosphere to be explained. Contributions of different sources into total $O_2(a^1\Delta_g, v = 0)$ molecules were obtained; the sensitivity of the retrieved ozone profile to variations of atmospheric components at different latitudes was studied. This model was also incomplete, because it did not include the triplet ozone photolysis channel, the process of resonance populating of the first singlet level of the $O_2(a^1\Delta_g, v = 0)$ oxygen molecule, and atomic oxygen quenching of $O(^1D)$ atoms.

Local sensitivity of the chemical model of tropospheric ozone was analyzed in Ref. 6 with accounting for interphase transitions (gas–liquid) depending on variations of atmospheric parameters. The model has many uncertainties in both chemical mechanism and input parameters (concentrations of basic atmospheric components), however, the authors have studied the sensitivity to not only individual variable parameters, but simultaneously a combination of several parameters. Together with a standard technique for sensitivity study with the help of relative error indices the authors used the dimensionless errors method.

The sensitivity of the two-dimensional model of ozone in the middle atmosphere (10–80 km) in night conditions depending only on the variations of chemical reaction rates was studied in Ref. 7. As a sensitivity characteristic, the dimensionless sensitivity coefficient was used. The formula was suggested connecting the ozone retrieval error with the factors of model sensitivity to individual reactions and given variations of reaction rate constants (5 or 10%). A group of key reactions, to which the vertical ozone profile retrieval is the most sensitive, was revealed from the analysis.

The technique[8] to study sensitivity of the $O(^1D)$ atom glow model in the 630 nm band in twilight conditions is suggested, which depends on three parameters:

a) the density of neutral atmospheric components (by doubling and halving corresponding concentrations);

b) the neutral meridional wind;

c) the variations of solar flux intensity.

The sensitivity of the model to variations of reaction rate constants was not analyzed as well.

Variations of a retrieved stratospheric ozone profile against different experimentally measured quantum yields of $O(^1D)$ atoms in the Hartley band were studied in Ref. 9.

The sensitivity of the new YM-2003 model has not been analyzed, hence, the purpose of this work is to study the model sensitivity to variations of:

1) the atmospheric component concentrations,

2) the gas temperature,

3) the chemical reaction rate constants,

for both the direct problem of $O_2(a^1\Delta_g, v \geq 0)$ and $O_2(b^1\Sigma_g^+, v \geq 0)$ concentrations calculation and the inverse one of vertical ozone profile retrieval from the emission intensities of Atm (0–0) and IR Atm (0–0) O_2 bands.

1. Sensitivity characteristics

In general case, the calculation results of excited component concentrations in the model of ozone and molecular oxygen photodissociation depend on all the model parameters: atmospheric component concentrations, photodissociation rate, constants of reaction rates, and quantum yields of the reactions' products. Denote the input parameters as x_i, the required function as f, variation of which at small variations of the input parameters can be presented as

$$df = \sum_i \frac{\partial f}{\partial x_i} dx_i. \quad (1)$$

Here summation is performed over all the input parameters.

From Eq. (1) obtain the relative error of f definition depending on the relative errors in setting input parameters x_i:

$$\frac{df}{f} = \sum_i \frac{\partial f}{\partial x_i} \frac{dx_i}{f} = \sum_i \frac{\partial \ln f}{\partial \ln x_i} \frac{dx_i}{x_i}, \quad (2)$$

where $\partial \ln f / \partial \ln x_i$ are the sensitivity coefficients S_i of the required function f depending on variations of the input parameter x_i under the condition of invariability of all the parameters x_j for $j \neq i$; dx_i/x_i is the relative error δ_i in setting input parameter x_i.

Thus, Equation (2) has a simple physical interpretation if to consider small variations of input parameters. The relative error of definition of the output parameter f is due to relative errors of input parameters x_i and sensitivity coefficients S_i, characterizing the properties of ozone and molecular oxygen photodissociation model:

$$\frac{\Delta f}{f} = \sum_i S_i \delta_i. \quad (3)$$

In contrast to the approach from Ref. 7, our approach is more general, because the error in the required parameter f definition in Eq. (3) is due to the measurement errors of all parameters from the ozone and molecular oxygen photolysis model.

Using the finite difference method, Equation (3) can be rewritten in the form[7]

$$S_i = \ln\left(f'/f\right) / \ln\left(x_i'/x_i\right). \quad (4)$$

The sensitivity coefficient S_i is a dimensionless number showing how much the required function f depends on variations of the input parameter x_i; in this case, consider $|S| > 1.0$ as a strong sensitivity, $0.1 < |S| < 1.0$ as a normal one, and $|S| < 0.1$ as a weak one.

The relative sensitivity Δ is used in the literature as an alternative. It is defined as the relative variation of some required parameter (e.g., ozone concentration) while varying a certain input parameter (e.g., the concentration of one of basic atmospheric components or the rate constant of a certain reaction):

$$\Delta = \frac{f'(x_i') - f(x_i)}{f(x_i)} 100\%, \tag{5}$$

where x_i and x_i' is the input (variable) parameter (initial value and its variation); f and f' is the required function (initial value and its variation).

Figure 2 illustrates both methods for sensitivity study with the help of: a) the relative sensitivity Δ and b) the sensitivity coefficient S.

As it is evident from Fig. 2, the method “a” is convenient because it allows one not only to define numerically the output-input parameter dependence but also its deviation (increase or decrease) by the variation sign; nevertheless, the method does not give clear understanding of whether this dependence is strong or weak (at a stronger variation of an input parameter we obtain a stronger variation of the output one).

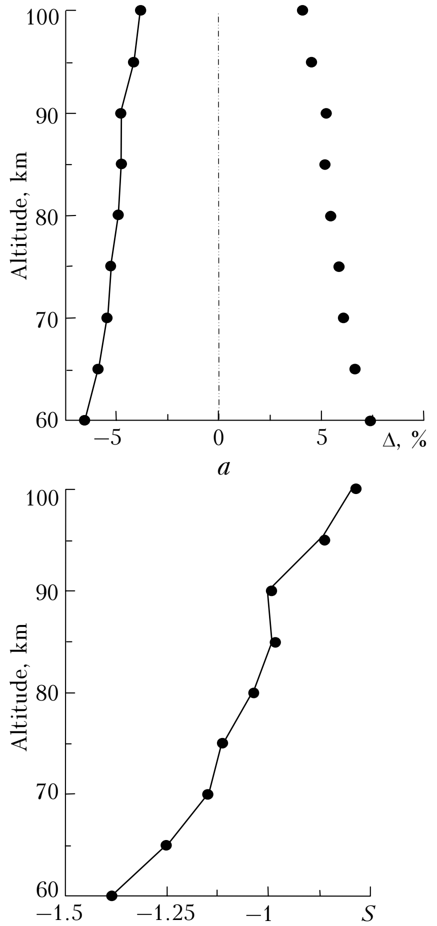

a

b

Fig. 2. The sensitivity of the calculated $O_2(b^1\Sigma_g^+, v = 0)$ concentration as a function of $[N_2]$ variations: the relative sensitivity Δ (dots correspond to the concentration decrease, lines with dots – to its increase) (*a*); dimensionless sensitivity coefficient S (dots correspond to the concentration decrease, lines – to its increase) (*b*).

The “b” method is more universal and its convenience is in the dimensionless sensitivity coefficient S, identically characterizing the dependence of the required parameter f on variations of the input parameter x_i (the vertical profile of $O_2(b^1\Sigma_g^+, v = 0)$ molecules concentration as a function of $[N_2]$ variations is shown in Fig. 2). Therefore, later on we use the sensitivity coefficient S in Tables and relative sensitivity Δ in Figures.

Note, that the sensitivity coefficient S_i at small variations of x_i is connected with the relative sensitivity Δ by the following equation:

$$S_i = \ln(\Delta_f + 1)/\ln(\Delta_{x_i} + 1), \tag{6}$$

where

$$\Delta_f = (f'/f) - 1, \quad \Delta_{x_i} = (x_i'/x_i) - 1.$$

It should be noted that small magnitude of the sensitivity coefficient S_i of variations of some input parameter (chemical reaction rate constants K_i, concentrations of atmospheric components $[O_2]$, $[N_2]$, $[O(^3P)]$, $[O_3]$, $[CO_2]$, gas temperature T_g) does not mean that it is of low unimportance and can be omitted from the model parameters, because it can have a large fractional error δ_i. The converse proposition is also valid: a processes with large sensitivity coefficient S_i can have so small relative error δ_i, that their contribution to the error of f definition can be negligible, as is follows from Eq. 3.

As it will be shown below, there is a series of processes, for which the dimensionless sensitivity is determined as weak in the direct problem (calculation of $O_2(b^1\Sigma_g^+, v)$ and $O_2(a^1\Delta_g, v)$ profiles) but they cannot be ignored in the inverse problem (O_3 retrieval).

In this work, the complete inspection of the YM-2003 model sensitivity to variations of atmospheric components $[O_2]$, $[N_2]$, $[O(^3P)]$, $[O_3]$, $[CO_2]$ concentrations, gas temperature T_g, and reaction rate constant K_i was performed in the direct problem:

– $O_2(b^1\Sigma_g^+, v)$ concentration calculation,

– $O_2(a^1\Delta_g, v)$ concentration calculation, as well as in the inverse one:

– vertical O_3 profile retrieval from the emission of Atm (0–0) O_2 band,

– vertical O_3 profile retrieval from the emission of IR Atm (0–0) O_2 band.

The conclusions were made on the basis on YM-2003 validation for different variations of atmospheric components, but for definiteness and consistency of estimates in Figures and Tables below variations of input parameters were used (Table 1).

Table 1. Values of δ_i variations in % and kinetic parameters in the YM-2003 model sensitivity analysis

$[O_2]$	$[N_2]$	$[O(^3P)]$	$[O_3]$	$[CO_2]$	T_g	K_i
±5	±5	±20	±20	±25	±15	±20

2. Direct problem: sensitivity analysis for calculated vertical profiles of concentrations of $O_2(b^1\Sigma_g^+, v)$ and $O_2(a^1\Delta_g, v)$ molecules

The direct problem is a possibility to calculate populations of all electronic-vibrational excited

$O_2(b^1\Sigma_g^+, v)$ and $O_2(a^1\Delta_g, v)$ oxygen levels, considered in the model, with known input parameters (concentration of basic atmospheric components, gas temperature, rate constants, and quantum yields of reactions). Three vibrational levels $v = 0$–2 are considered for $O_2(b^1\Sigma_g^+, v)$ level and six levels $v = 0$–5 – for $O_2(a^1\Delta_g, v)$ one (see Fig. 1).

In this part, sensitivity curves are given only for $v = 0$ level of the $O_2(b^1\Sigma_g^+)$ and $O_2(a^1\Delta_g)$ molecules, the results for $v \geq 1$ are given in Table 2.

Figure 3 shows Δ values for $O_2(b^1\Sigma_g^+, v = 0)$ concentration depending on variations of atmospheric component concentrations and temperature (see Table 1).

Table 2. Sensitivity coefficients *S* for the direct problem of $O_2(b^1\Sigma_g^+, v)$ and $O_2(a^1\Delta_g, v)$ concentrations calculation

Variable parameter	Sensitivity coefficient		
	$\|S\| > 1.0$	$0.1 < \|S\| < 1.0$	$\|S\| < 0.1$
$[O_2]$	(*b*, 0)	(*b*, 1–2), (*a*, 0–5)	
$[N_2]$	(*b*, 0)	(*b*, 1), (*a*, 0)	(*b*, 2), (*a*, 1–5)
[O]		(*b*, 0,2), (*a*, 0)	(*b*, 1), (*a*, 1–5)
$[CO_2]$			(*b*, 0–2), (*a*, 0–5)
$[O_3]$		(*b*, 0–1), (*a*, 0–5)	(*b*, 2)
T_g	(*b*, 1–2)	(*b*, 0), (*a*, 0)	(*a*, 1–5)
$O(^1D) + O_2 \rightarrow$ products		(*b*, 0–1)	
$O_2(b, 2) + O \rightarrow O_2(b, 1) + O$		(*b*, 2)	(*b*, 1)
$O_2(b, 2) + O_2 \rightarrow O_2(X, 2) + O_2(b, 0)$		(*b*, 2)	(*b*, 0)
$O_2(b, 2) + N_2 \rightarrow O_2(b, 1) + N_2$			(*b*, 1–2)
$O_2(b, 2) + O_3 \rightarrow 2O_2 + O$			(*b*, 2)
$O_2(b, 1) + O \rightarrow O_2(b, 0) + O$			(*b*, 0–1)
$O_2(b, 1) + O_2 \rightarrow O_2(X, 1) + O_2(b, 0)$		(*b*, 1)	(*b*, 0)
$O_2(b, 1) + N_2 \rightarrow O_2(b, 0) + N_2$		(*b*, 1)	(*b*, 0)
$O_2(b, 1) + O_3 \rightarrow 2O_2 + O$			(*b*, 0–1)
$O_2(b, 0) + O \rightarrow$ products		(*b*, 0)	(*a*, 0)
$O_2(b, 0) + O_2 \rightarrow$ products			(*b*, 0), (*a*, 0)
$O_2(b, 0) + N_2 \rightarrow$ products		(*b*, 0)	(*a*, 0)
$O_2(b, 0) + O_3 \rightarrow$ products			(*b*, 0), (*a*, 0)
$O_2(b, 0) + CO_2 \rightarrow O_2(a, 0) + CO_2$			(*b*, 0), (*a*, 0)
$O_2(a, v \geq 1) + O \rightarrow O_2 + O$			(*a*, 1–5)
$O_2(a, v \geq 1) + O_2 \rightarrow O_2(X, v) + O_2(a, 0)$		(*a*, 1–5)	(*a*, 0)
$O_2(a, v \geq 1) + N_2 \rightarrow O_2(a, 0) + N_2$			(*a*, 0–5)
$O_2(a, 0) + O \rightarrow O_2 + O$			(*a*, 0)
$O_2(a, 0) + O_2 \rightarrow$ products		(*a*, 0)	
$O_2(a, 0) + N_2 \rightarrow O_2 + N_2$			(*a*, 0)
$O_2(a, 0) + O_3 \rightarrow O_2 + O_3$			(*a*, 0)

Note. (*b*, 0–2) – $O_2(b^1\Sigma_g^+, v = 0–2)$, (*a*, 0–5) – $O_2(a^1\Delta_g, v = 0–5)$.

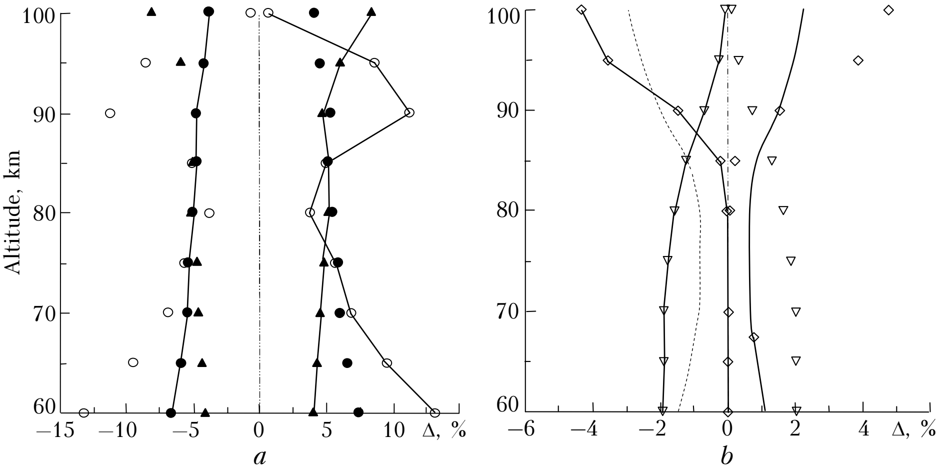

Fig. 3. Relative sensitivity of the calculated $O_2(b^1\Sigma_g^+, v = 0)$ concentrations as a function of variations of atmospheric parameters. Symbols correspond to decreasing concentration of atmospheric components: $[O_2]$ is black triangles, $[N_2]$ is black circles, $[O_3]$ is empty circles (*a*); [O] is rhombus, $[CO_2]$ is apex-down triangles (*b*). Lines with corresponding symbols represent the concentration increase. The dashed line corresponds to the relative sensitivity when T_g decreasing and the solid one – when T_g increasing.

For convenience, Figure 3*a* shows large numerical values of the relative sensitivity Δ and Figure 3*b* – small ones.

Figure 4 shows Δ values for $O_2(b^1\Sigma_g^+, v = 0)$ concentration against variations of rate constants of the most essential reactions (see Table 1).

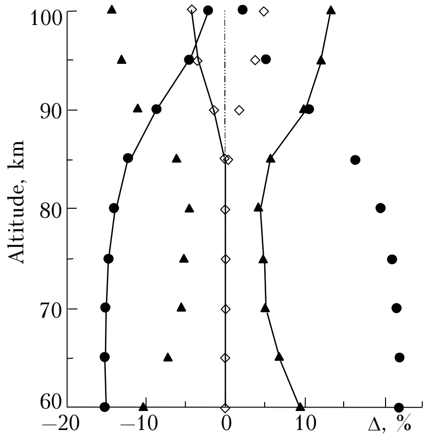

Fig. 4. Relative sensitivity of the calculated $O_2(b^1\Sigma_g^+, v = 0)$ concentration as a function of variations of reaction rate constants. Symbols correspond to the decrease of the constants $(O(^1D) + O_2 \rightarrow$ – black triangles, $O_2(b^1\Sigma_g^+, v = 0) + O \rightarrow$ – rhombus, $O_2(b^1\Sigma_g^+, v = 0) + N_2 \rightarrow$ – black circles); lines with corresponding symbols – to their increase.

The relative sensitivity of $O_2(b^1\Sigma_g^+, v = 0)$ concentration variations has not exactly linear character, which is especially evident from Fig. 3: the $O_2(b^1\Sigma_g^+, v = 0)$ concentration sensitivity changes much more stronger as the reaction rate constant $O_2(b^1\Sigma_g^+, v = 0) + N_2 \rightarrow$ decreases then as it increases.

Figures 5 and 6 show Δ values for $O_2(b^1\Sigma_g^+, v = 0)$ concentration against variations of concentrations of atmospheric components, temperature, and reaction rate constants (see Table 1).

The conducted analysis allowed us to reveal processes playing an important role in calculation of $O_2(b^1\Sigma_g^+, v)$ and $O_2(a^1\Delta_g, v)$ concentrations. For the direct problem of $O_2(b^1\Sigma_g^+, v)$ calculation, there is a strong sensitivity for the vibrational level $v = 0$ against variations of $[O_2]$ and $[N_2]$ concentrations and for the levels $v = 1$ and 2 – against the gas temperature T_g variations. Processes, strongly sensitive to variations of atmospheric parameters and rate constants, were not revealed for the direct problem of $O_2(a^1\Delta_g, v)$ calculation. The majority of processes have either standard or weak sensitivity in $O_2(b^1\Sigma_g^+, v)$ and $O_2(a^1\Delta_g, v)$ calculations.

3. Inverse problem: sensitivity analysis of vertical O_3 profile retrieval from the intensities of the Atm (0–0) and IR Atm (0–0) O_2 bands

The inverse problem is a possibility to calculate one or several model input parameters (including concentrations of trace atmospheric components

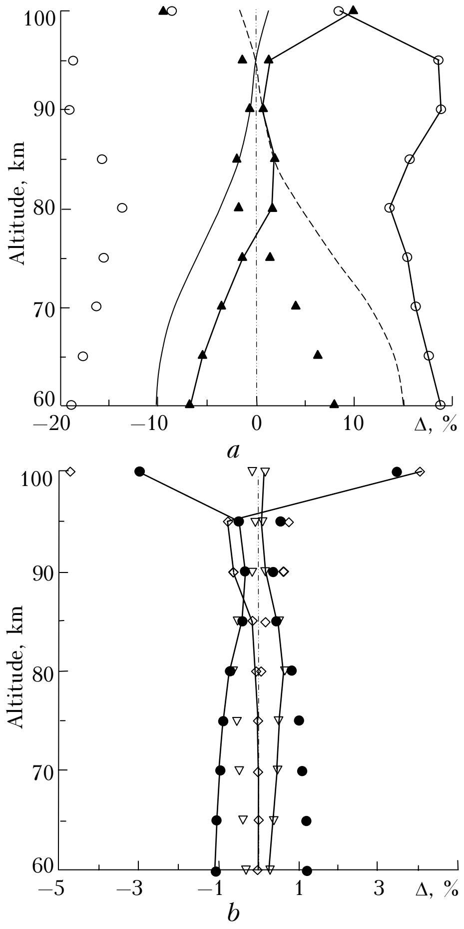

Fig. 5. Relative sensitivity of the calculated $O_2(a^1\Delta_g, v = 0)$ concentrations as a function of atmospheric parameters variations. Symbols correspond to decrease of concentration of atmospheric components: $[O_2]$ – black triangles, $[O_3]$ – empty circles (*a*); $[N_2]$ – black circles, [O] – rhombus, $[CO_2]$ – apex-down triangles (*b*). Lines with corresponding symbols represent the concentration increase. The dashed line corresponds to the relative sensitivity when T_g decreases and the solid one – when it increases.

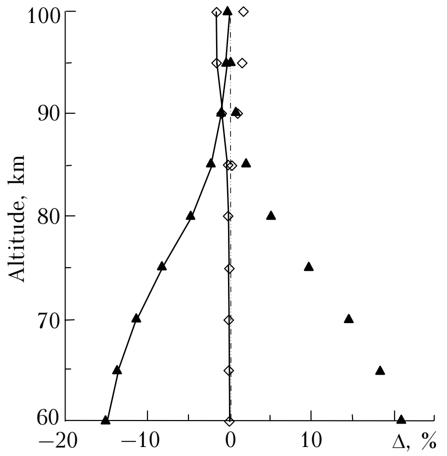

Fig. 6. Relative sensitivity of the calculated $O_2(a^1\Delta_g, v = 0)$ concentration as a function of variations of reaction rate constants. Symbols correspond to the decrease of the constants $(O_2(a^1\Delta_g, v = 0) + O_2 \rightarrow$ – black triangles, $O_2(a^1\Delta_g, v = 0) + O \rightarrow$ – rhombus); lines with corresponding symbols – to their increase.

$[O_3]$ and $[O(^3P)]$) from the intensities of measured emissions (e.g., oxygen molecule emission) on the assumption all other input parameters known, including the model of the atmospheric and processes proceeding in it.

In this section, the results of sensitivity analysis of vertical ozone profile retrieval from the measurements of O_2 emission intensities at 762 nm and 1.27 μm depending on variations of atmospheric parameters and reaction rate constants.

Figures 7 and 8 show Δ values for the problem of ozone concentration profile retrieval from the emission intensity of the Atm (0–0) (762 nm) O_2 band depending on variations of atmospheric components, the temperature, and rate constants of some reactions and Figures 9 and 10 are for the IR Atm (0–0) (1.27 μm) O_2 band (see Table 1).

Similarly to the direct problem of the relative sensitivity analysis, the relative sensitivity depends nonlinearly on variations of atmospheric parameters and rate constants for the above inverse problem.

The results of sensitivity analysis of vertical O_3 profile retrieval from the intensities of emissions of the Atm (0–0) and IR Atm (0–0) O_2 bands are given in Table 3.

The analysis revealed a series of processes important for the solution of the inverse problem of ozone concentration retrieval. An $[O_3]$ profile retrieved from the intensity of emission of the Atm (0–0) O_2 band is extremely sensitive to variations of vertical profiles of $[O_2]$ and $[N_2]$ concentrations and essentially depends on the rate constant of the reaction $O_2(b^1\Sigma_g^+, v = 0) + N_2 \rightarrow$ products. There were not revealed processes with high sensitivity to variations of atmospheric parameters and rate constants in the inverse problem for IR Atm (0–0) O_2 band. The majority of the processes in both inverse problems have either standard or weak sensitivity.

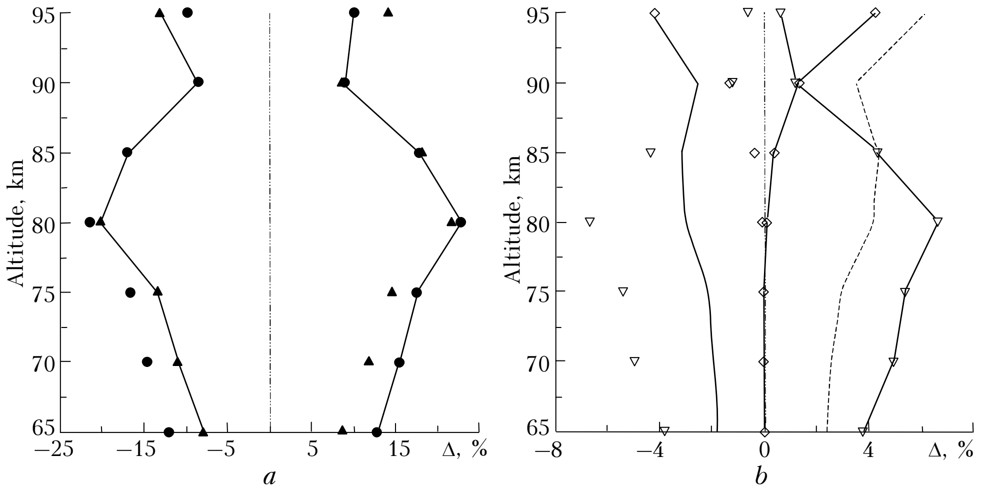

a *b*

Fig. 7. Relative sensitivity of vertical ozone profile retrieval from the intensity of Atm (0–0) O_2 (762 nm) emission as a function of variations of atmospheric parameters. Symbols correspond to decrease of concentration of atmospheric components: $[O_2]$ – black triangles, $[N_2]$ – black circles (*a*); [O] – rhombus, $[CO_2]$ – apex-down triangles (*b*). Lines with corresponding symbols represent the concentration increase. The dashed line corresponds to the relative sensitivity as T_g decreases and the solid one – as it decreases.

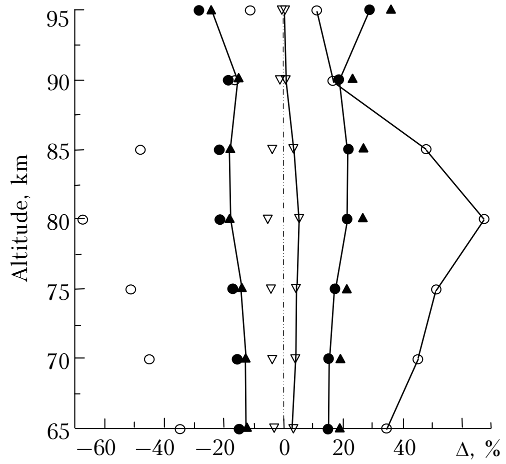

Fig. 8. Relative sensitivity of vertical ozone profile retrieval from the intensity of Atm (0–0) O_2 emission as a function of variations of reaction rate constants. Symbols correspond to the decrease of the constants ($O(^1D) + O_2 \rightarrow$ – black triangles, $O(^1D) + N_2 \rightarrow$ – black circles, $O_2(b^1\Sigma_g^+, v = 0) + N_2 \rightarrow$ – empty circles, $O_2(b^1\Sigma_g^+, v = 0) + CO_2 \rightarrow$ – apex-down triangles); lines with corresponding symbols – to their increase.

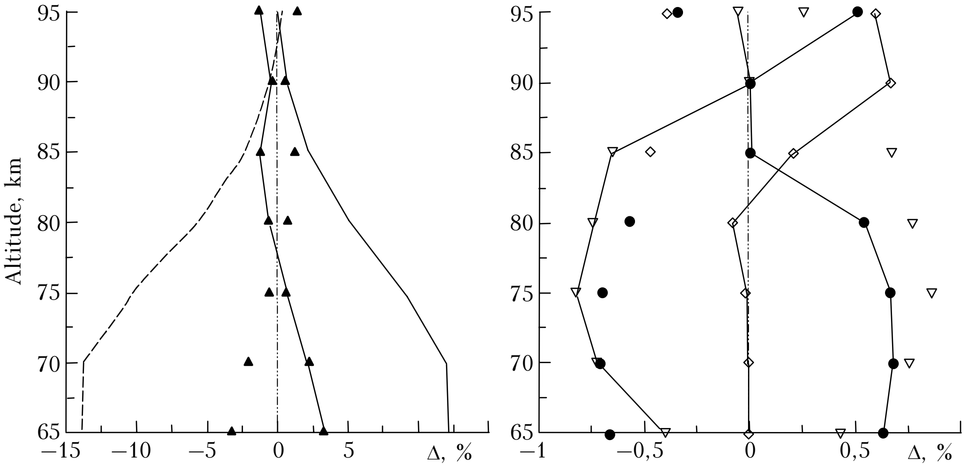

a *b*

Fig. 9. Relative sensitivity of ozone vertical profile retrieval from the intensity of IR Atm (0–0) O_2 emission as a function of variations of atmospheric parameters. Symbols correspond to decrease of concentration of atmospheric components: $[O_2]$ – black triangles (*a*); $[N_2]$ – black circles, $[O]$ – rhombus, $[CO_2]$ – apex-down triangles (*b*). Lines with corresponding symbols represent the concentration increase. The dashed line corresponds to the relative sensitivity when T_g decreasing and the solid one – when decreasing.

Table 3. Sensitivity coefficient *S* for the inverse problem of ozone concentration vertical profile retrieval

Variable parameter	Sensitivity coefficient		
	$\|S\| > 1.0$	$0.1 < \|S\| < 1.0$	$\|S\| < 0.1$
1	2	3	4
$[O_2]$	Atm	IR Atm	
$[N_2]$	Atm	IR Atm	
$[O]$			Atm, IR Atm
$[CO_2]$		Atm	IR Atm
T_g		Atm, IR Atm	
$O(^1D) + O \rightarrow 2O$			Atm
$O(^1D) + O_2 \rightarrow$ products		Atm	
$O(^1D) + N_2 \rightarrow$ products		Atm	
$O_2(b, 2) + O \rightarrow O_2(b, 1) + O$			Atm
$O_2(b, 2) + O_2 \rightarrow O_2(X, 2) + O_2(b, 0)$			Atm
$O_2(b, 2) + N_2 \rightarrow O_2(b, 1) + N_2$			Atm
$O_2(b, 2) + O_3 \rightarrow 2O_2 + O$			Atm
$O_2(b, 1) + O \rightarrow O_2(b, 0) + O$			Atm
$O_2(b, 1) + O_2 \rightarrow O_2(X, 1) + O_2(b, 0)$			Atm
$O_2(b, 1) + N_2 \rightarrow O_2(b, 0) + N_2$			Atm
$O_2(b, 1) + O_3 \rightarrow 2O_2 + O$			Atm
$O_2(b, 0) + O \rightarrow$ products			Atm, IR Atm
$O_2(b, 0) + O_2 \rightarrow$ products			Atm, IR Atm
$O_2(b, 0) + N_2 \rightarrow$ products	Atm		IR Atm
$O_2(b, 0) + O_3 \rightarrow$ products			Atm, IR Atm
$O_2(b, 0) + CO_2 \rightarrow O_2(a, 0) + CO_2$		Atm	IR Atm
$O_2(a, v \geq 1) + O \rightarrow O_2 + O$			IR Atm
$O_2(a, v \geq 1) + O_2 \rightarrow O_2(X, v) + O_2(a, 0)$			IR Atm
$O_2(a, v \geq 1) + N_2 \rightarrow O_2(a, 0) + N_2$			IR Atm
$O_2(a, 0) + O \rightarrow O_2 + O$			IR Atm
$O_2(a, 0) + O_2 \rightarrow$ products		IR Atm	
$O_2(a, 0) + N_2 \rightarrow O_2 + N_2$			IR Atm
$O_2(a, 0) + O_3 \rightarrow O_2 + O_3$			IR Atm

Note. Atm, IR Atm – O_3 retrieval from the intensities of emissions of Atm (0–0) and IR Atm (0–0) O_2 bands, respectively.

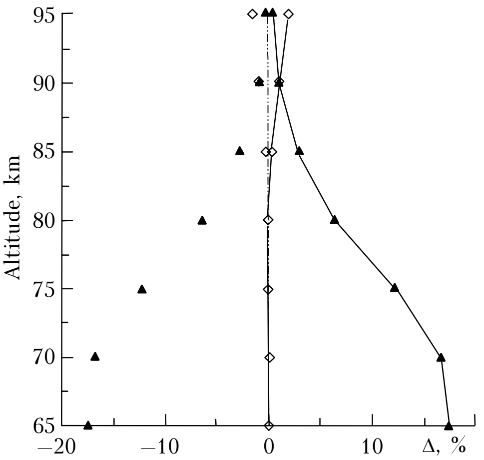

Fig. 10. Relative sensitivity of ozone vertical profile retrieval from the intensity of IR Atm (0–0) O_2 emission as a function of variations of reaction rate constants. Symbols correspond to the decrease of the constants ($O_2(a^1\Delta_g, v = 0) + O_2 \rightarrow$ – triangles, $O_2(a^1\Delta_g, v = 0) + O \rightarrow$ – rhombus); lines with corresponding symbols – to their increase.

4. Discussion

Quite evident dependence of the calculated profiles of electronic-vibrationally excited oxygen molecules and ozone profiles, retrieved from different molecular oxygen emissions, on variations of atmospheric components is revealed from the conducted analysis of YM-2003 model sensitivity (see Tables 2 and 3), as well as the group of 10 reactions mostly influencing the calculations in the direct and inverse problems. Table 4 presents the most recent data on rate constants of these reactions along with the errors from the references.

Rate constants of the principal reactions (Table 4), revealed from the above analysis, are sufficiently accurate measured: measurement error δ for the constants $K_1 - K_3$ and $K_6 - K_{10}$ does not exceed 20% (as was assumed in Table 1); just for the constants K_4 and K_5 the errors are 37 and 30%, respectively. The contribution of the reaction $O_2(b^1\Sigma_g^+, v = 1) + O_2 \rightarrow O_2(X^3\Sigma_g^-, v = 1) + O_2(b^1\Sigma_g^+, v = 0)$ is significant in the direct problem ($S_4\delta_4 = 0.30$ near the mesopause) while the reaction $O_2(b^1\Sigma_g^+, v = 0) + O \rightarrow$ contributes insignificantly in the direct problem due to low sensitivity of the model to this reaction ($S_5\delta_5 = 0.021$ maximally near the mesopause). However, note that the value of this rate constant has not been measured and the value, given in Table 4, is estimating.[13]

The reaction $O(^1D) + O_2 \rightarrow$ is the main light emission source at λ = 762 nm in daytime mesosphere and lower thermosphere in the transition $O_2(b^1\Sigma_g^+, v = 0) \rightarrow O_2(X^3\Sigma_g^-, v = 0)$. Its rate constant K_1 is well-known (the error does not exceed 8%). It is commonly thought that the $O_2(b^1\Sigma_g^+, v = 0)$ molecules are formed in this reaction, though it was recently shown experimentally[16] that the quantum yield of these molecules in this reaction does not exceed 0.2 and the yield of $O_2(b^1\Sigma_g^+, v = 1)$ molecules is about 0.8. In other words, the main part of products of this reaction is formed in the electronic-vibrationally excited state. The effective rate of $O_2(b^1\Sigma_g^+, v = 0)$ molecule formation and the vertical profile of the volume emission rate of the 762 nm O_2 atmospheric band can be calculated only with accounting for electronic-vibrational kinetics of O_2, described in the new YM-2003 model. This mechanism is important for both direct and inverse problems.

The reaction of $O_2(b^1\Sigma_g^+, v = 0)$ quenching by molecular nitrogen is one of key reactions in the problem of ozone retrieval from the 762 nm emission intensity ($S_6\delta_6 = 0.13$–0.48 in the mesosphere). However, there is a problem of determining the quantum yield of the reaction products for this reaction. Different ways of the reaction of $O_2(b^1\Sigma_g^+, v = 0)$ quenching by N_2 molecules should be considered within the YM-2003 model of electronic-vibrational kinetics of O_2 and O_3. In Ref. 5, quantum yield of the reaction

$$O_2(b^1\Sigma_g^+, v = 0) + N_2 \rightarrow O_2(a^1\Delta_g, v = 0) + N_2(X, v = 2) + 607.1 \text{ cm}^{-1} \quad (7)$$

is supposed to be 1.

The rate constant of this reaction is virtually 100 times as much as the rate constant of the reaction of $O_2(b^1\Sigma_g^+, v = 0)$ decontamination by molecular oxygen.

Table 4. Rate constants of the reactions most important for the YM-2003 model

Reaction	Reaction rate constants K, $cm^3 \cdot s^{-1}$	Ref.
$O(^1D) + O_2 \rightarrow$ products	$K_1 = (3.12 \pm 0.25) \cdot 10^{-11} e^{(70\pm10)/T}$	[10]
$O(^1D) + N_2 \rightarrow$ products	$K_2 = (2.1 \pm 0.2) \cdot 10^{-11} e^{(115\pm10)/T}$	[10]
$O_2(b, 2) + O_2 \rightarrow O_2(X, 2) + O_2(b, 0)$	$K_3 = (1.2 \pm 0.2) \cdot 10^{-11} e^{-(596\pm100)/T}$	[11]
$O_2(b, 1) + O_2 \rightarrow O_2(X, 1) + O_2(b, 0)$	$K_4 = (2.2 \pm 0.8) \cdot 10^{-11}(T/292)^{1.0\pm0.3} e^{-(115\pm105)/T}$	[12]
$O_2(b, 0) + O \rightarrow$ products	$K_5 = (8.0 \pm 2.4) \cdot 10^{-14}$	[13]
$O_2(b, 0) + N_2 \rightarrow$ products	$K_6 = (2.03 \pm 0.30) \cdot 10^{-15} e^{-(37\pm40)/T}$	[14]
$O_2(b, 0) + CO_2 \rightarrow O_2(a, 0) + CO_2$	$K_7 = (3.39 \pm 0.36) \cdot 10^{-13}$	[14]
$O_2(a, v > 1) + O_2 \rightarrow$ products	$K_8 = (3.6 \pm 0.4) \cdot 10^{-11}$	[15]
$O_2(a, 1) + O_2 \rightarrow O_2(X, 1) + O_2(a, 0)$	$K_9 = (5.6 \pm 1.1) \cdot 10^{-11}$	[15]
$O_2(a, v = 0) + O_2 \rightarrow$ products	$K_{10} = (3.0 \pm 0.6) \cdot 10^{-18} e^{-(200\pm200)/T}$	[13]

Note. $O_2(b^1\Sigma_g^+, v)$ – $O_2(b, v)$, $O_2(a^1\Delta_g, v)$ – $O_2(a, v)$, $O_2(X^3\Sigma_g^-, v)$ – $O_2(X, v)$.

In view of relatively large rate constant of this reaction, the assumption was made[17] that proceeding of this reaction is of quasi-resonance process type:

$$O_2(b^1\Sigma_g^+, v = 0) + N_2 \to O_2(a^1\Delta_g, v = 2) + N_2(X, v = 1) - 31.9\ \text{cm}^{-1}. \quad (8)$$

One more quasi-resonance process is also possible:

$$O_2(b^1\Sigma_g^+, v = 0) + N_2 \to O_2(X^3\Sigma_g^-, v = 9) + N_2(X, v = 0) - 52.8\ \text{cm}^{-1}. \quad (9)$$

There is no data on possible quantum yields of products of this reaction in channels (8) and (9). These two quasi-resonance processes exist simultaneously, and we suppose that they have similar quantum yields.

The constants K_8 and K_9 were measured recently. Though the model sensitivity to these reactions is significant ($S \sim 0.9$), their maximal contribution $S\delta$ into the error for direct and inverse problems does not exceed 0.19. Other reactions (see Tables 2 and 3) have small sensitivity coefficients and small errors of reaction rate constants, that does not distort calculations within the framework of both direct and inverse problems.

Thus, among 10 reactions (Table 4), revealed by the model sensitivity analysis, only two reactions, i.e., $O_2(b^1\Sigma_g^+, v = 0) + N_2 \to$ and $O_2(b^1\Sigma_g^+, v = 1) + O_2 \to O_2(X^3\Sigma_g^-, v = 1) + O_2(b^1\Sigma_g^+, v = 0)$, can significantly increase the error of vertical ozone profile retrieval. Evidently, new measurements of the rate constants of these reactions are required.

Conclusions

The sensitivity analysis of the model of electronic-vibrational kinetics of O_2 and O_3 in the Earth's middle atmosphere has been carried out. The equation connecting the calculation error of output parameters (in the direct and inverse problems) and the coefficients of the model sensitivity to input parameters and relative errors of these parameters have been obtained. The following conclusion has been made from the analysis:

1. The vertical profile of $O_2(b^1\Sigma_g^+, v = 0)$ concentration strongly depends on $[O_2]$ and $[N_2]$ profiles, in contrast to $O_2(b^1\Sigma_g^+, v \geq 1)$ and $O_2(a^1\Delta_g, v \geq 0)$ ones.
2. [O] and $[O_3]$ variations result in insignificant variations of $O_2(b^1\Sigma_g^+, v \geq 0)$ and $O_2(a^1\Delta_g, v \geq 0)$ profiles while $[CO_2]$ variations are virtually negligible.
3. T_g variations result in strong variations of $O_2(b^1\Sigma_g^+, v \geq 1)$ concentration profiles and insignificant variations of $O_2(b^1\Sigma_g^+, v = 0)$ and $O_2(a^1\Delta_g, v \geq 0)$ profiles.
4. Calculations of $O_2(b^1\Sigma_g^+, v = 2)$ concentration are sensitive to the rate constants of the reactions $O_2(b^1\Sigma_g^+, v = 2) + M$ (where M = O or O_2) $\to$, of $O_2(b^1\Sigma_g^+, v = 1)$ concentration – to the rate constants of the reactions $O(^1D) + O_2 \to$ and $O_2(b^1\Sigma_g^+, v = 1) + O_2 \to$, of $O_2(b^1\Sigma_g^+, v = 0)$ concentration – to the rate constants of the reactions $O(^1D) + O_2 \to$ and $O_2(b^1\Sigma_g^+, v = 0) + M$ (where M = O or N_2) $\to$.
5. Calculations of $O_2(a^1\Delta_g, v \geq 0)$ concentration are sensitive to the rate constants of the reactions $O_2(a^1\Delta_g, v \geq 0) + O_2 \to$.
6. The accuracy of ozone concentration retrieval from the emission intensity of the Atm (0–0) O_2 band strongly depends on variations of $[O_2]$ and $[N_2]$ concentrations, in addition, the dependence on variations of the vertical profile of $[CO_2]$ concentration has been revealed.
7. Significant dependences on variations of atmospheric components and model parameters in retrieval of ozone concentration vertical profile from the emission intensity of the IR Atm (0–0) O_2 band have not been revealed.
8. An essential role of the reaction $O_2(b^1\Sigma_g^+, v = 0) + N_2 \to$ was revealed for O_3 concentration retrieval from the emission intensity of Atm (0–0) O_2 band.

Acknowledgements

This work was supported by the Russian Foundation for Basic Researches (Grant No. 05–05–65318).

References

1. V.A. Yankovsky and R.O. Manuilova, Atmos. Oceanic Opt. **16**, No. 7, 536–540 (2003).
2. V.A. Yankovsky and R.O. Manuilova, Ann. Geophys. **24**, No. 11, 2823–2839 (2006).
3. V.A. Yankovsky and V.A. Kuleshova, Atmos. Oceanic Opt. **19**, No. 7, 514–518 (2006).
4. R.J. Sica, Can. J. Phys. **69**, Nos. 8–9, 1069–1075 (1991).
5. M.G. Mlynczak, S.C. Solomon, and D.S. Zaras, J. Geoph. Res. D **98**, No. 10, 18639–18648 (1993).
6. Y. Zhang, C.H. Bischof, R.C. Easter, and Wu Po-Ting, J. Geophys. Res. D **103**, No. 15, 18953–18979 (1998).
7. L. Chen, H. Rabitz, D.B. Considine, C.H. Jackman, and J.A. Shorter, J. Geophys. Res. D **102**, No. 13, 16201–16214 (1997).
8. D.J. Melendez-Alvira, D.G. Torr, P.G. Richards, W.R. Swift, M.R. Torr, T. Baldridge, and H. Rassoul, J. Geophys. Res. A **100**, No. 5, 7839–7853 (1995).
9. N. Taniguchi, S. Hayshida, K. Takahashi, and Y. Matsumi, Atmos. Chem. Phys., No. 3, 1293–1300 (2003).
10. A.R. Ravishankara, E.J. Dunlea, M.A. Blitz, T.J. Dillon, D.E. Heard, M.J. Pilling, R.S. Strekowski, J.M. Nicovich, and P.H. Wine, Geophys. Res. Lett. **29**, No. 15, 35–38 (2002).
11. K.S. Kalogerakis, R.A. Copeland, and T.G. Slanger, J. Chem. Phys. **116**, No. 12, 4877–4885 (2002).
12. D.A. Pejakovic, E.R. Wouters, K.E. Phillips, T.G. Slanger, R.A. Copeland, and K.S. Kalogerakis, J. Geophys. Res. **110**, A03308, doi: 10.1029/2004JA010860 (2005).
13. R. Atkinson, D.L. Baulch, R.A. Cox, J.N. Crowley, R.F. Hampson, R.G. Hynes, M.E. Jenkin, M.J. Rossi, and J. Troe, Atmos. Chem. Phys., No. 4, 1461–1738 (2004).
14. E.J. Dunlea, R.K. Talukdar, and A.R. Ravishankara, J. Phys. Chem. A **109**, No. 17, 3912–3920 (2005).
15. T.G. Slanger and R.A. Copeland, Chem. Rev. **103**, No. 12, 4731–4766 (2003).
16. J.G. Green, J. Shi, and J.R. Barker, J. Phys. Chem. A **104**, No. 26, 6218–6226 (2000).
17. M. Braithwaite, J.A. Davidson, and E.A. Ogryzlo, J. Chem. Phys. **65**, No. 2, 771–778 (1976).